Available online at www.sciencedirect.com
ScienceDirect
Chemical Physics Letters 443 (2007) 76–81
CHEMICAL PHYSICS LETTERS
www.elsevier.com/locate/cplett

Location of conical intersections in solution using a sequential quantum mechanics/molecular dynamics method

Aurora Muñoz Losa, M. Elena Martín, Ignacio Fdez. Galván, Manuel A. Aguilar *

Departamento de Química Física, Universidad de Extremadura, Avda. de Elvas s/n, 06071 Badajoz, Spain

Received 14 February 2007; in final form 4 June 2007
Available online 13 June 2007

Abstract

An extended version of the ASEP/MD method oriented to the study of the solvent effects on the structural and energetic properties of minimal energy crossing points between different potential energy surfaces is presented. The method, based on an extension of Bearpark's proposal to the case of solvated molecules, permits to locate conical intersections and intersystem crossings both in equilibrium and non-equilibrium solvent conditions. As an application we studied the *s-trans*-acrolein $^1(n \rightarrow \pi^*)$ singlet–singlet conical intersection in aqueous solution. The ground and excited state surfaces of the solute molecule are described at CASSCF level while the solvent structure is obtained from molecular dynamics simulations.

1. Introduction

Non-adiabatic processes [1] (processes that imply more than one potential energy surface) play a key role in molecular spectroscopy and chemical reaction dynamics. In the last years, the study and characterization of this type of processes has received much attention, among other reasons because they explain a large amount of radiationless decays and isomerization processes of polyatomic α molecules [2].

Most theoretical studies performed to date on non-adiabatic processes have addressed the study of conical intersections (CI) and intersystem crossing (ISC) in gas phase conditions using both semiempirical [3,4] and ab initio methods [5–9], and only recently the interest has been shifted to the study of processes in solution [10–12]. The reasons are obvious, to the difficulties inherent to the location of surface crossings in vacuo one must add the complications associated to the presence of a solvent, that is, the great number of solvent molecules that interact with the solute molecule and the existence of a manifold of configurations thermally accessible that must be included to obtain statistically significant results.

Several recent studies have proposed methods to introduce solvent effects in the search of CI points. Burghardt et al. [10,11], for instance, use continuum methods to study CI in solution considering equilibrium and non-equilibrium solvation. In the first case the solvent follows in every moment the changes originated in the solute charge distribution during the photochemical process. On the contrary, in non-equilibrium conditions the solvent structure is fixed (usually in the structure corresponding to the equilibrium with the solute ground state). The consideration of non-equilibrium solvation is motivated by the fact that most radiationless relaxations take place on the femtoseconds time scale, a scale in which, probably, the solvent equilibration is not complete. Methods that permit a more detailed description of the solvent have also been proposed, so, in a recent paper, Yamazaki and Kato [12] use the RISM-SCF method for describing energy surface crossing in ethylene and $CH_2NH_2^+$ in polar solvents under non-equilibrium conditions. Finally, several groups [13–15] have used QM/MM methods to locate CI generally in non-equilibrium conditions.

* Corresponding author.
E-mail addresses: jellby@unex.es (I.Fdez. Galván), maguilar@unex.es (M.A. Aguilar).

0009-2614/$ - see front matter © 2007 Elsevier B.V. All rights reserved.
doi:10.1016/j.cplett.2007.06.037

In this letter, we present a method to locate and to describe the energetic and geometrical properties of unavoided crossings of potential energy surfaces in solution both in equilibrium and non-equilibrium conditions. The proposed method is an extension to the case of solvated molecules of an algorithm due to Bearpark et al. [7], which permits to locate the lowest energy point of the conical intersection seam without employing Lagrange multipliers. The method is valid for all types of crossings (although in this letter, we restrict ourselves to the case of CI) and combines a high level ab-initio quantum-mechanical description of the solute with a detailed description of the solvent obtained through molecular dynamics (MD) simulations.

2. Method

In a conical intersection the degeneracy between the two intersecting surfaces is lifted linearly in displacements from the intersection. The subspace of nuclear coordinates in which the degeneracy is lifted is named the branching space or g–h plane [1]. Two vectors define this plane, the difference gradient vector ($\vec{g}_{KJ}$):

$$\vec{g}_{KL} = \nabla(E_K - E_L) \tag{1}$$

and the non-adiabatic coupling vector ($\vec{h}_{KL}$):

$$\vec{h}_{KL} = \langle \Psi_K | \nabla | \Psi_L \rangle \tag{2}$$

where the gradient ∇ is a vector in the nuclear space and Ψ_I are the adiabatic electronic wave functions, eigenfunctions of the electronic Hamiltonian, H, with energies E_i.

Following the algorithm proposed by Bearpark et al. [7], to locate a minimal energy crossing point one must simultaneously minimize the difference between the two intersecting states K and L and the energy of the upper state K along the $(N-2)$-dimensional seam [3]. The direction followed during the optimization is given by the vector [7]:

$$\vec{f}_{KL} = 2(E_K - E_L)\hat{g}_{KL} + \left[\nabla E_k - (\nabla E_K \cdot \hat{g}_{KL})\hat{g}_{KL} - \left(\nabla E_K \cdot \hat{h}_{KL}\right)\hat{h}_{KL}\right] \tag{3}$$

Here, $\hat{g}_{KL}$ and $\hat{h}_{KL}$ are the versors defined as $\hat{g}_{KL} = \vec{g}_{KL}/|\vec{g}_{KL}|$ and $\hat{h}_{KL} = \vec{h}_{KL}/|\vec{h}_{KL}|$, respectively. The first and second terms on the rhs of this equation do not have the same physical dimensions. The reason is that the function minimized is $(E_K - E_L)^2$ [7,3]. This function varies more smoothly than $(E_K - E_L)$ in the vicinity of a conical intersection and is more suitable for quasi-Newton optimization methods [3].

In our model, the 'in solution' energies and wavefunctions of the solute intersecting states are obtained using the averaged solvent electrostatic potential from molecular dynamics data method (ASEP/MD) [16–20].

As in QM/MM methods, in ASEP/MD, the energy and state function of the solvated solute molecule are obtained by solving the effective Schrödinger equation:

$$H|\Psi = (H_{QM} + H_{QM/MM})|\Psi = E|\Psi \tag{4}$$

Where H_{QM} is the 'in vacuo' solute molecular Hamiltonian and where the solute–solvent interaction term, $H_{QM/MM}$ takes the following form:

$$H_{QM/MM} = H^{elect}_{QM/MM} + H^{vdw}_{QM/MM} \tag{5}$$

$$H^{elect}_{QM/MM} = \int \mathrm{d}r \cdot \hat{\rho} \cdot \langle \widehat{V}_S(r;\rho) \rangle \tag{6}$$

where $\hat{\rho}$ is the solute charge density and the brackets denote a statistical average. The term $\langle \widehat{V}_S(r) \rangle$ is the averaged electrostatic potential generated by the solvent at the position r, and is obtained from MD calculations where the solute molecule is represented by the charge distribution ρ and a geometry fixed during the simulation. For details about the calculation of $\langle \widehat{V}_S(r) \rangle$, see references [16,17]. The term $H^{vdw}_{QM/MM}$ is the Halmiltonian for the van der Waals interaction, in general represented by a Lennard–Jones potential. This term is calculated averaging its value over all the solvent configurations selected during the MD simulation. It depends only on the nuclear coordinates and hence has no effect on the solute wave function but it contributes to the final value of the gradient and Hessian.

The scheme of the process followed to locate CI or ISC of molecules in solution using ASEP/MD is shown in Fig. 1. First, one must obtain an in vacuo set of charges for the solute molecule in its initial state, generally the ground state. These charges are then used as input for an MD simulation of the solute–solvent molecules, the remaining solute (LJ coefficients) and solvent (charges and LJ coefficients) parameters are obtained from the literature. N representative solvent configurations (N usually taken between 500 and 1000) are selected from the MD simulation. From these configurations the averaged solvent potential generated by the solvent in the volume occupied by the solute, $\langle \widehat{V}_S(r) \rangle$, is calculated. Next, one solves the electronic Schrödinger equation of the solute molecule in the presence of the averaged perturbation generated by the solvent. The different energies and gradients appearing in Eq. (3), that now include explicitly the solvent effect, together with a new set of solute charges are calculated and the gradient $\vec{f}$ is obtained. Finally, a new solute geometry is obtained by using a Newton-Raphson method. In this point we have two possibilities depending on whether the solvent is in an equilibrium or non-equilibrium situation. In the first case the solvent must become equilibrated with the new solute charge distribution and hence a new MD must be performed. Although strictly speaking it is necessary to perform a MD calculation for each new solute geometry, this is a very inefficient procedure. We have verified that it is computationally more efficient to perform several steps of the CI searching procedure before equilibrating again the solvent. We update the solvent structure only after 10–20 iterations of the search procedure.

In the case of non-equilibrium conditions, the CI is located for a fixed solvent structure. One supposes that during an electron transition the Franck–Condon principle is applicable and the solvent nuclei remain fixed during the

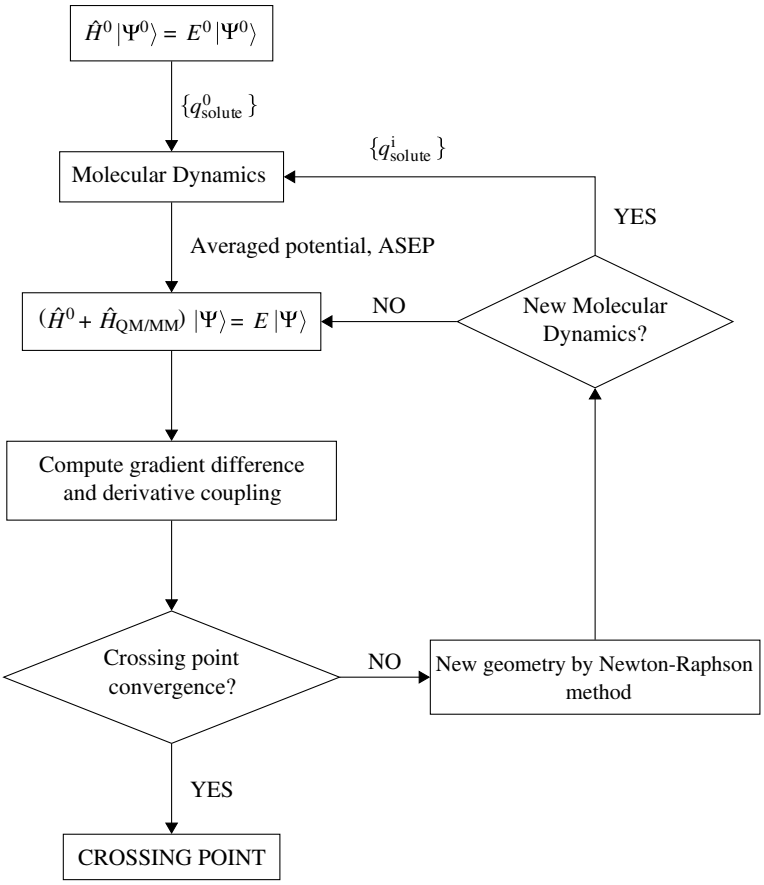

Fig. 1. CI and ISC location scheme.

transition, that is, the solvent is in equilibrium with the minimum energy structure of the solute ground state.

In this scheme we introduce furthermore the following approximations:

(1) Electrostatic and Lennard–Jones (LJ) solute–solvent contributions are treated in different ways. Thus, while the electrostatic component is introduced as a perturbation into the solute Hamiltonian, and hence it affects both the energy and the wavefunction, it is assumed that the LJ contribution depends only on the nuclear coordinates, and hence, for a given solute geometry, it is a constant added to the energy. This component does not affect the solute wavefunctions.
(2) It is supposed that the LJ parameters are the same in the ground and excited states, in consequence their contribution to $\vec{g}_{\text{KL}}$ cancels out. The LJ component only contributes to the excited state gradient. On the contrary, the electrostatic contribution influences the calculation of the gradient difference, $\vec{g}_{\text{KL}}$, of the derivative coupling, $\vec{h}_{\text{KL}}$, and of the excited state gradient, ∇E_{K}.

For in solution systems, the CI are defined on free energy surfaces. Because of this, once the geometry of the CI has been located with ASEP/MD, one must determine the free energy difference between the CI point and a reference state, generally the Franck–Condon state or the minimum of the ground state. The standard free-energy difference between initial (reference) and final (CI) states in solution can be written as the sum of two terms [20]

$$\Delta G_{\text{diff}} = \Delta E_{\text{solute}} + \Delta G_{\text{int}}, \tag{7}$$

where

$$\Delta E_{\text{solute}} = E^{\text{f}} - E^{\text{i}} = \langle \psi^{\text{f}}|H_{\text{QM}}|\psi^{\text{f}}\rangle - \langle \psi^{\text{i}}|H_{\text{QM}}|\psi^{\text{i}}\rangle \tag{8}$$

is the ab initio difference between the two quantum mechanics, QM, states calculated using the in vacuo solute molecular Hamiltonian, $\widehat{H}_{\text{QM}}$, and the electronic wavefunctions obtained in solution.

In Eq. (7), ΔG_{int} is the difference in the solute–solvent interaction free energy between the two QM states. The free-energy perturbation method [21] was used to determine this energy. The solute geometry was assumed to be rigid and a function of the perturbation parameter (λ) while the solvent was allowed to move freely. When $\lambda = 0$ the solute geometry and charges and the solute–solvent correspond to the initial state. When $\lambda = 1$ the charges, LJ parameters, and geometry are those of the final state. For intermediate values a linear interpolation is applied. A value of $\Delta\lambda = 0.05$ was used. That means that a total of 21 separate molecular dynamics simulations were carried

out to determine the free energy difference. To test the convergence of the calculation, the difference in interaction free energies calculated forwards and backwards was compared.

3. Computational details

We have studied the S_0/S_1 $^1(n \rightarrow \pi^*)$ crossing of *s-trans*-acrolein in solution considering equilibrium and non-equilibrium conditions. The states were described using the CASSCF level of theory. In previous Letters [22,23] it was shown that the inclusion of the dynamic correlation component through CASPT2 calculations was compulsory if one desired to reproduce the transition energy. However, in the acroleine case this component does not modify the solvent shift [23] and a good description of the solvent effects can be obtained at CASSCF level. The complete active space was spanned by all the configurations arising from six valence electrons in five orbitals (6*e*/5*o*). All quantum calculations were performed with the program GAUSSIAN 98 [24] and using the 6-31G* basis set. The initial geometry for acrolein was obtained by CASSCF optimization both in vacuum and in solution with the aforementioned basis set. In all the cases we take as initial point of the CI search procedure, the geometry of the Franck–Condon (FC) excitation, i.e., the geometry of the ground state minimum.

To locate the CI we used a Newton-Raphson method where the increment of geometry h is defined by

$$h = -\sum_{i=1}^{n} \frac{\mathbf{v}_\mathbf{i}^\mathbf{t}\mathbf{g}\mathbf{v}_\mathbf{i}}{b_\mathrm{i}} \tag{9}$$

here, $\mathbf{v_i}$ and b_i are the eigenvectors and the eigenvalues, respectively, of the Hessian matrix and $\mathbf{g}$ the gradient described previously. To update the approximate Hessian, we employed the Broyden–Fletcher–Goldfarb–Shanno (BFGS) algorithm. We consider that the CI has been reached when the energy difference between the two states is lower than 0.002 a.u. (~1.3 kcal/mol) and the energy and geometry are stabilized. The minimal energy CI (MECI) is the lowest energy point that fulfils these conditions. In solution the results are affected by statistical uncertainty and we take averaged values of the last five ASEP/MD cycles.

The MD calculations were performed using the program MOLDY [25]. A total of 251 molecules were simulated with fixed intramolecular geometry by combining LJ interatomic interactions (see Table 1) with electrostatic interactions. The solvent was represented by 250 TIP3P [26,27] molecules with fixed intramolecular geometry in a cubic box of 18.7 Å side. Periodic boundary conditions were applied, and spherical cutoffs were used to truncate the molecular interactions at 9.0 Å. A time step of 0.5 fs was used. The electrostatic interaction was calculated with the Ewald method. The temperature was fixed at 298 K by using a Nosé–Hoover thermostat. Each MD calculation simulation was run for 75 ps (25 ps equilibration, 50 ps production).

Table 1
Lennard–Jones parameters

	σ (Å)	ε (kcal/mol)
H_2–H_3–H_4	2.42	0.030
C_2–C_3	3.55	0.076
C_1	3.75	0.105
O	2.96	0.210
H_1	2.42	0.015
O (W)	3.15	0.608
H (W)	0.00	0.000

4. Results

As example of application of the method developed in previous sections, we proceeded to localized the S_0/S_1 $^1(n \rightarrow \pi^*)$ CI of *s-trans*-acrolein. In vacuum, the MECI is placed about 20.0 kcal/mol higher than the S_1 minimum and 1.6 kcal/mol over the S_1 FC point, see Fig. 2 and Table 2. Our results are similar to those obtained by Reguero et al. [8] (values in parentheses) with bond distances for the MECI of 1.49 (1.49), 1.30 (1.30) and 1.39 (1.40) Å for the C=C, C–C and C=O bonds, respectively. The energy difference between the two intersecting states is in our case of only 0.1 kcal/mol (2.0 kcal/mol).

The geometry of the FC and MECI calculated for the in vacuo system are displayed in Fig. 2. The comparison between the MECI geometry and the Franck–Condon point evidences the interchange between single and double bonds: in the CI the C_3=C_2 and C_1=O distances increase while the C_1—C_2 distance decreases. The rupture of the

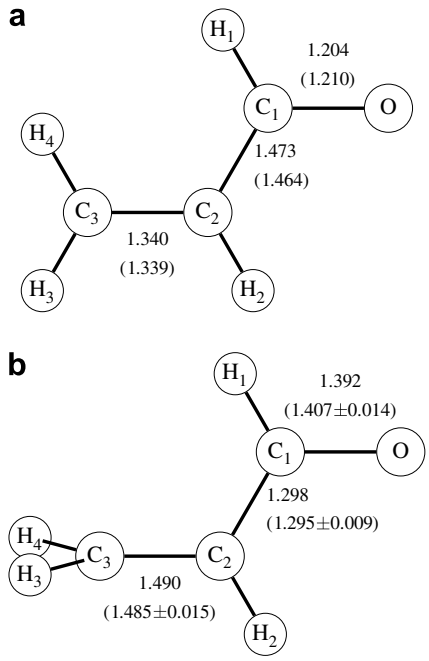

Fig. 2. (a) FC geometry in vacuo and in solution (in parenthesis). (b) The CI S_0/S_1 geometry in vacuo and in solution (in parenthesis). Distances in Å.

Table 2
Absolute (in a.u.) and relative (in kcal/mol) energies and its components in different points of the S1 excited state surface in vacuum and in solution

	Vacuum	ΔE (vac)	ΔG_{diff}	ΔE_{solute}	ΔG_{int}
S_0 minimum	−190.8235	0.0	0.0	0.0	0.0
S_1 $^1(n \rightarrow \pi^*)$ minimum	−190.7081	72.4	75.1	71.1	4.0
S_1 $^1(n \rightarrow \pi^*)$ FC	−190.6788	90.8	95.8	89.7	6.1
S_0/S_1 $^1(n \rightarrow \pi^*)$ CI	−190.6762	92.4	94.5	91.3	3.2

C_3=C_2 double bond facilitates the rotation of the C_1–C_2–C_3–H_3 angle as far as 100°. At the same time there is a flux of charge from the C_3=C_2 bond to the C_1=O bond, consequently the dipole moment value increases in about 146% with respect to the FC value, see Table 3.

Next, we calculated the CI in aqueous solution supposing an equilibrium situation. Fig. 3 displays the variation of the energies of the two states involved along the search procedure. The solvent originates a solvent shift in the absorption band of 5.0 kcal/mol very close to the results obtained with larger basis sets [22] and to the experimental [28] value, 4.5 kcal/mol. It also modifies the relative position of the CI that now is 1.3 kcal/mol under the S_1 FC point and 19.04 kcal/mol over the S_1 minimum. Consequently, the conical intersection is easier to reach in solution than in gas phase. There are no appreciable differences between the bond distances obtained in vacuo and in solution conditions. As expected, the solvent increases the dipole moment values but more so in FC point than in the CI and the S_1 minimum, consequently the variations of the dipole moment on the S_1 surface are lower in solution than

Table 3
Dipole moment values in Debyes

	Vacuum	Solution
S_0 minimum	2.88	3.94 ± 0.04
S_1 $^1(n \rightarrow \pi^*)$ minimum	1.55	1.84 ± 0.08
S_1 $^1(n \rightarrow \pi^*)$ FC	1.05	1.87
S_0/S_1 $^1(n \rightarrow \pi^*)$		
S_1 $^1(n \rightarrow \pi^*)$	2.59	3.06 ± 0.05
S_0	1.78	2.13 ± 0.08

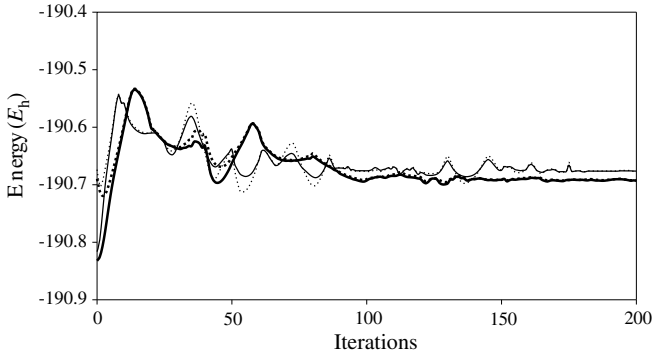

Fig. 3. Evolution during the search procedure of the S_0 and S_1 energies (in hartree) in vacuum (thin lines, continuous and dotted, respectively), and in solution (thick lines, continuous and dotted, respectively).

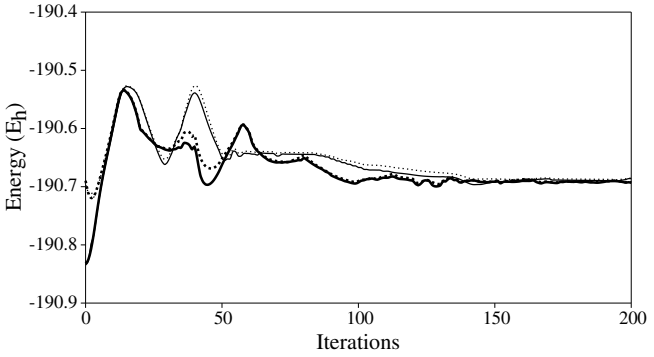

Fig. 4. Evolution during the search procedure of the S_0 and S_1 energies (in hartree) in solution in non-equilibrium (thin lines, continuous and dotted, respectively) and in equilibrium conditions (thick lines, continuous and dotted, respectively).

in gas phase. This fact explains the small influence of the solvent on the relative stability of this CI.

In acrolein, the molecular shape does not vary appreciably during the evolution from the FC to the CI geometries. In these conditions it is possible to reach the CI keeping the solvent structure fixed (non-equilibrium conditions) although now it is somewhat more complicated to localize the CI, see Fig. 4. The CI is now 3.2 kcal/mol over the FC point, that is, the CI is destabilized 4.5 kcal/mol with respect to the equilibrium solvation situation. The effect of non-equilibrium solvation on the geometry follows a trend similar to the previously obtained with the solvent in equilibrium: the C_1=O distances increases while the C_3=C_2 and C_1–C_2 distances decrease. The bond distances are now 1.478 Å (C_3=C_2), 1.411 Å (C_1=O) and 1.287 Å (C_1–C_2).

5. Conclusions

A new method to locate CI and ISC in solution has been presented, the method permits to combine high level quantum calculations in the solute description with a detailed description of the solvent structure obtained from molecular dynamics simulations. Furthermore, the method can be used with the solvent in equilibrium and non-equilibrium conditions. As an example of application we have studied the solvent effect on the S_0/S_1 $^1(n \rightarrow \pi^*)$ CI in *s-trans*-acrolein. This crossing is not the most probable path of photochemical de-excitation for acrolein, [29] because it is located slightly above the FC point, but it can serve to illustrate the solvent effect on free energy surface crossings.

As expected, the solvent polarizes the molecule and increases the dipole moment values in the different geometries: FC, CI and ground and excited state minima. The differential solvation between the ground and excited state produces a blue shift on the absorption band of 5.0 kcal/mol. The variations of the dipole moment along the S_1 surface are small, consequently the solvent has only a small effect on the relative position of the MECI. In equilibrium solvent conditions, the CI is slightly easier to reach than in

vacuo, however when one fixes the solvent (non-equilibrium solvation) the MECI is destabilized by almost 4.5 kcal/mol.

Acknowledgement

This work was supported by the CTQ2004-05680 Project from the Ministerio de Educación y Ciencia of Spain.

References

[1] D.R. Yarkony, in: W. Domcke, D.R. Yarkony, H. Köppel (Eds.), Conical Intersections, Advances Series in Physical Chemistry, vol. 15, World Scientific, Singapore, 2004, p. 42.
[2] M. Olivucci, A. Sinicropi, in: M. Olivucci (Ed.), Computational Photochemistry, vol. 16, Elsevier, Amsterdam, 2005.
[3] A. Toniolo, M. Ben-Nun, T.J. Martinez, J. Phys. Chem. A 106 (2002) 4679.
[4] C. Ciminelli, G. Granucci, M. Persico, Chem. Eur. J. 10 (2004) 2327.
[5] D.R. Yarkoni, J. Chem. Phys. 92 (1990) 2457.
[6] N. Ragazos, M.A. Robb, F. Bernardi, M. Olivucci, Chem. Phys. Lett. 197 (1992) 217.
[7] M.J. Bearpark, M.A. Robb, H.B. Schlegel, Chem. Phys. Lett. 223 (1994) 269.
[8] M. Reguero, M. Olivucci, F. Bernardi, M.A. Robb, J. Am. Chem. Soc. 116 (1994) 2103.
[9] M.E. Martín, F. Negri, M. Olivucci, J. Am. Chem. Soc. 126 (2004) 5452.
[10] I. Burghardt, L. Cederbaum, T. Hynes, Farad. Discuss. 127 (2004) 395.
[11] R. Spezia, I. Burghardt, J. Hynes, Mol. Phys. 5–7 (2006) 903.
[12] S. Yamazaki, S. Kato, J. Chem. Phys. 123 (2005) 114510.
[13] A. Toniolo, G. Granucci, T.J. Martinez, J. Phys. Chem. A 107 (2003) 3822.
[14] M. Garavelli, F. Rugen, F. Ogliano, M.J. Bearpark, F. Bernardi, M. Olivucci, M.A. Robb, J. Comp. Chem. 24 (2003) 1357.
[15] L.M. Frutos, T. Andruniów, F. Santoro, N. Ferré, M. Olivucci, Proc. Natl. Acad. Sci. U.S.A. 104 (2007) 7764.
[16] M.L. Sánchez, M.A. Aguilar, F.J. Olivares del Valle, J. Comput. Chem. 18 (1997) 313.
[17] I. Fdez. Galván, M.L. Sánchez, M.E. Martín, F.J. Olivares del Valle, M.A. Aguilar, J. Chem. Phys. 118 (2003) 255.
[18] I. Fdez. Galván, M.L. Sánchez, M.E. Martín, F.J. Olivares del Valle, M.A. Aguilar, Comput. Phys. Commun. 155 (2003) 244.
[19] I. Fdez. Galván, F.J. Olivares del Valle, M.E. Martín, M.A. Aguilar, Theor. Chem. Acc. 111 (2004) 196.
[20] I. Fdez. Galván, M.E. Martín, M.A. Aguilar, J. Comp. Chem. 25 (2004) 1227.
[21] P.A. Kollman, Chem. Rev. 93 (1993) 2395.
[22] M.E. Martín, A. Muñoz Losa, I. Fdez. Galván, M.A. Aguilar, J. Chem. Phys. 121 (2004) 3710.
[23] A. Muñoz Losa, I. Fdez. Galván, M.E. Martín, M.A. Aguilar, J. Phys. Chem. B 110 (2006) 19064.
[24] M.J. Frisch, G.W. Trucks, H.B. Schlegel, et al., GAUSSIAN 98, Gaussian, Inc., Pittsburgh, PA, 1998.
[25] K. Refson, Comput. Phys. Commun. 126 (2000) 310.
[26] W.L. Jorgensen, D.S. Maxwell, J. Tirado-Rives, J. Am. Chem. Soc. 117 (1996) 11225.
[27] W.L. Jorgensen, J. Chandrasekhar, J.D. Madura, R.W. Impey, M.L. Klein, J. Chem. Phys. 79 (1983) 926.
[28] A.E. Moskvin, Theor. Exp. Chem. 2 (1966) 175.
[29] The most probable path of de-excitation involves several ISC and CI crossings.